Available online at www.sciencedirect.com
ScienceDirect
Sensors and Actuators A 145–146 (2008) 330–335
SENSORS AND ACTUATORS A PHYSICAL
www.elsevier.com/locate/sna

Electrical and electromechanical characteristics of self-assembled carbon nanotube thin films on flexible substrates

Wei Xue [a,b], Tianhong Cui [a,*]

[a] *Department of Mechanical Engineering, University of Minnesota, Minneapolis, MN 55455, USA*
[b] *Department of Mechanical Engineering, Washington State University, Vancouver, WA 98686, USA*

Received 29 June 2007; received in revised form 4 November 2007; accepted 17 December 2007
Available online 3 January 2008

Abstract

We report the fabrication and characterization of layer-by-layer self-assembled single-walled carbon nanotube (SWNT) thin films on plastic substrates. The SWNT multilayers are alternating layers of SWNTs and poly(dimethyldiallylammonium chloride) (PDDA). The SWNTs are deposited on the pre-patterned gold electrodes and measured as thin-film resistors. The resistance of the SWNT thin film decreases when the number of assembled SWNT layers increases. The SWNT layers are modeled as a set of resistors in parallel with a “base” resistor and “layer” resistors. The flexibility of the polymer substrate allows high bending angles. We discovered that increasing the substrate bending angle greatly decreases the resistance of the SWNT thin film. For thin-film resistors (length: 2.8 cm) containing 14 and 16 SWNT layers, the resistance changes are measured as −38.2% and −47.1% at a bending height of 1 cm. The observed “piezoresistive” phenomenon of the assembled SWNT thin films creates opportunities for highly sensitive sensors and electronic devices in many areas.

Keywords: Single-walled carbon nanotube (SWNT); Thin film; Layer-by-layer (LbL) self-assembly; Flexible substrates

1. Introduction

The development of microelectromechanical systems (MEMS) has achieved great progress in the past 20 years [1]. Silicon is the dominant material for most microsystems. However, since the application areas have been broadened, silicon is not always the best material choice: silicon is expensive, brittle, and only available in specific shapes; silicon-based fabrication techniques need expensive instruments and cleanroom environment; and silicon is incompatible with many chemical and biological substances. Presently, research work about polymer electronics and polymer MEMS is growing rapidly. Polymers offer a number of advantages for microsystems: low material cost for high-volume fabrication; polymers are flexible and transparent; wide ranges of material properties and surface chemistries are available; and polymers are chemically and biologically compatible. It is believed that polymer integrated circuits (ICs) will take the place of silicon ICs in the low-end applications in the future.

The increasingly miniaturized micro/nano electronic devices and systems require smaller structural dimensions. Devices at nanometer scale represent the trend of fabrication and commercialization. Nanoscale materials including nanoparticles, nanowires, carbon nanotubes (CNTs), and biomolecules fulfill the requirements of nanofabrication and can be used for the development of innovative devices [2,3]. Among them, single-walled carbon nanotubes (SWNTs) have attracted tremendous attention due to their outstanding electrical and mechanical properties. Compared with traditional semiconducting materials, SWNTs demonstrate higher carrier mobility and better performance [4,5]. However, the process of producing individual SWNT devices is often time-consuming, and it requires complicated procedure and expensive equipment. In contrast, thin films composed of random network or aligned array of SWNTs are easily to produce and can be a good alternative [6]. SWNT multilayer can be produced in several hours with the “bottom-up” layer-by-layer (LbL) self-assembly technique, which is a low-cost and low-temperature approach for thin film deposition [7]. The thickness of the SWNT multilayer thin film can be

* Corresponding author at: Department of Mechanical Engineering, University of Minnesota, Twin Cities, 111 Church Street SE, Minneapolis, MN 55455, USA. Tel.: +1 612 626 1636; fax: +1 612 625 6069.
E-mail address: tcui@me.umn.edu (T. Cui).

0924-4247/$ – see front matter © 2008 Elsevier B.V. All rights reserved.
doi:10.1016/j.sna.2007.12.021

controlled from nanometer to micrometer scale [8]. Moreover, research shows that the SWNT thin films can be electrically continuous over large areas and therefore enhance the reliability of the devices [9].

We recently reported the deposition and characterization of SWNTs on silicon substrates [10,11]. The thin films are built with alternating layers of SWNTs and poly(dimethyldiallylammonium chloride) (PDDA, a positively charged polyelectrolyte). SWNTs are negatively charged by covalently attached carboxylic groups (–COOH) after being treated with nitric and sulfuric acids [12]. The assembly of SWNTs provides a low-cost, low-temperature, and solution-based technique to produce ultrathin films with a short process time. In this paper, we assemble SWNTs on flexible substrates and explore the electrical properties of the SWNT thin films. The cost of the thin-film devices is further reduced. In order to characterize their electrical properties, the SWNT thin films are assembled on pre-patterned Au electrodes. Relatively high numbers ($\geq$10) of SWNT layers are assembled on the substrates to ensure the interconnection between the metallic SWNTs. With an increasing number of the assembled SWNT layers, the resistance of the resistor decrease nonlinearly. Due to the high flexibility of the plastic substrate, we are able to bend the substrates at high angles. The resistance of the SWNT resistor decreases when the device is bent. The phenomenon and the underlying principles are described and discussed. Based on the "piezoresistive" phenomenon, a number of high-sensitivity sensors and electronic devices can be produced for a variety of applications.

2. Experiments

The pristine SWNT powder was purchased from Chengdu Organic Chemicals Co. Ltd. The average diameter and length of the SWNTs are 1.1 nm and 50 μm, respectively. To increase the solubility, the pristine SWNTs were first treated with nitric and sulfuric acids (1:3 HNO_3:H_2SO_4) at 100 °C for 45 min, and followed by filtration and ultrasonic vibration in deionized (DI) water. After the chemical functionalization process, the SWNTs are negatively charged and uniformly dispersed in DI water. More details in material preparation can be found in our previous report [12].

The creation of the SWNT resistors began with gluing a piece of off-the-shelf plastic transparency film on a 4-in. silicon wafer. Metal layers of Cr/Au (1000 Å/2000 Å) were electron-beam evaporated on the substrate and patterned as electrode pads using the conventional silicon surface-micromachining techniques including spin coating, UV lithography, photoresist development, and metal wet etching. An SWNT multilayer thin film composed of $(PDDA/SWNT)_n$ was deposited on the substrate and covered the whole surface, where n represents the number of coated layers. The SWNT thin film was coated using a "bottom-up" technique called layer-by-layer self-assembly. PDDA is a positively charged polyelectrolyte and the functionalized SWNTs have negative charges on the sidewalls and open ends; therefore, they can be held together by electrostatic force and form stable thin films. The $(PDDA/SWNT)_n$ multilayer was built in a repeated fashion by a "positive–negative–positive" charge alternation. The thickness of a (PDDA/SWNT) bi-layer is approximately 7.6 nm, reported previously by our group [10]. The fabrication of the SWNT thin films is very controllable, although there is a large degree of SWNT randomness in the resulting film. The schematic structure of the thin-film resistor is shown in Fig. 1. The width w and the length l of the resistor are 1 and 6 mm, respectively.

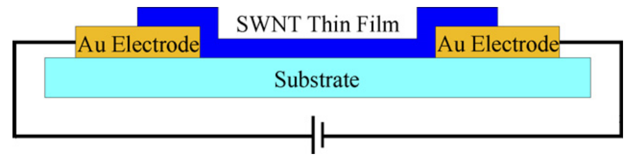

Fig. 1. Schematic structure of an SWNT thin-film resistor built on a flexible substrate.

Fig. 2a shows a transparency film with patterned Cr/Au electrodes. The optically transparent property of the film offers

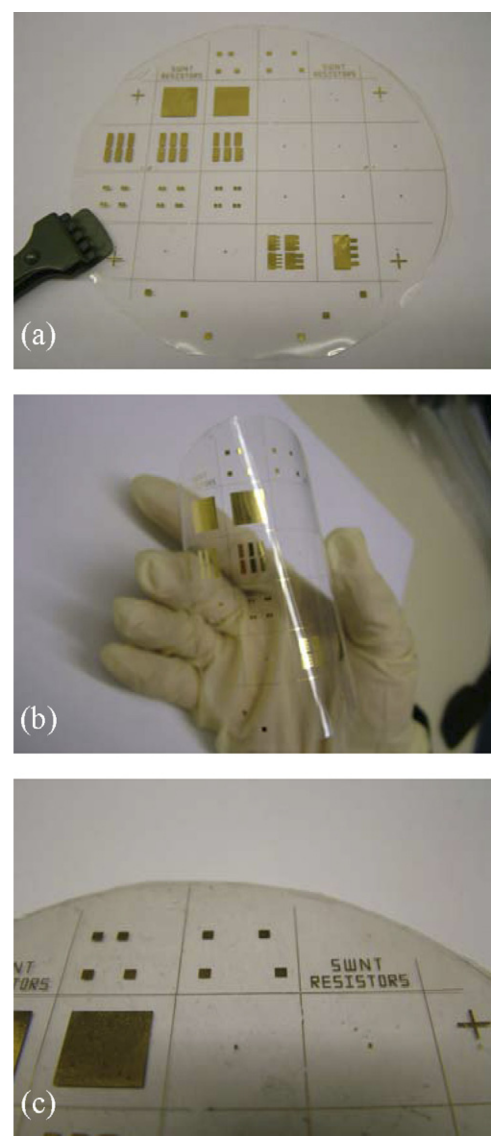

Fig. 2. (a) Patterned Cr/Au electrodes on a transparency substrate, (b) flexed transparency film and (c) transparency film coated with 5 layers of SWNTs.

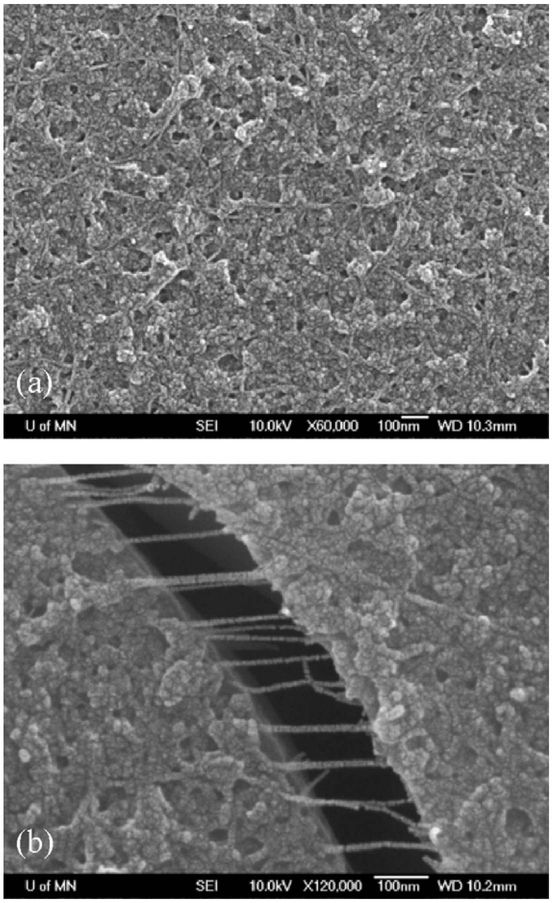

Fig. 3. High-resolution SEM images of self-assembled SWNTs.

advantages such as easy assembly and easy fault diagnosis of the devices. The transparency film is highly flexible, as shown in Fig. 2b. Moreover, there is no observed degradation in their resistance after repeated flexure. The transparency film gets darker as more SWNT layers are coated. Fig. 2c shows an optical image of the substrate coated with 5 SWNT layers. The high-resolution scanning electron microscope (SEM) images of the self-assembled SWNTs are illustrated in Fig. 3. The nanotubes are randomly grown on the surface and form a continuous network (Fig. 3a) on the substrate. The stretching of the thin film or the substrate causes "cracks" of the SWNT thin film. The SWNTs are stretched in between the gap and are still able to maintain the continuity of the thin film due to their high aspect ratios (Fig. 3b).

3. Electrical characteristics

The self-assembled SWNT thin-film resistors were characterized with an HP 4156A semiconductor parameter analyzer. Fig. 4a shows the measurement results of resistors with 10, 12, 14, 16 and 18 SWNT layers. All resistors demonstrate highly linear properties in the range of −2 to 2 V. The calculated resistances are $R = 3.56$, 1.57, 0.70, 0.24 and 0.17 MΩ, respectively. Since the SWNTs are randomly coated on the substrate and the resistance of the resistors can vary in a wide range, we fabricated a number of SWNT resistors on the flexible substrates and calculated the average resistances of these devices. The average resistances from 12 measurements are calculated as $R = 6.37$, 0.73, 0.30, 0.21 and 0.14 MΩ for resistors with $n = 10$, 12, 14, 16 and 18, respectively. The resistance decreases dramatically when n increases from 10 to 12. The decrease becomes relatively small after $n \geq 12$ (Fig. 4b). The scattered squares in the figure represent the measured results while the line represents the theoretical fit from the model shown in Fig. 5. The assembled SWNT thin films were also characterized using the four-point probe technique. Thin films with less than 10 SWNT layers were detected as insulators due to their high resistance. For $(PDDA/SWNT)_n$ multilayer with $n \geq 12$, the shape of the resistivity–number (ρ_r–n) curve from the four-point probe measurement is similar to that of the resistance–number (R–n) curve from the current–voltage (I–V) characterization (Fig. 4b, inset). The resistivity ρ_r of the SWNT multilayer is in the range of 0.5–2 Ω cm, which is similar to silicon with a doping concentration of approximately 10^{16} cm^{-3} [13].

In the LbL self-assembly process, the SWNTs are deposited in a repeated fashion. Each (PDDA/SWNT) bi-layer con-

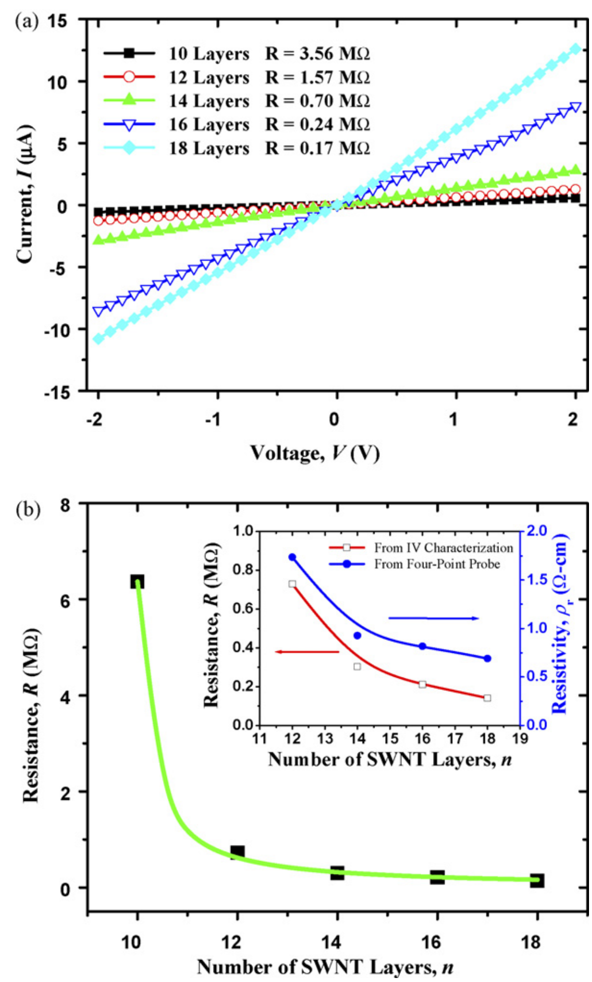

Fig. 4. Characteristics of SWNT thin-film resistors on flexible substrates. (a) Experimental current–voltage (I–V) curves of the thin-film resistors and (b) calculated average resistance (R) vs. the number of coated SWNT layers (n). The inset shows the results from the I–V characteristics as well as the four-point probe.

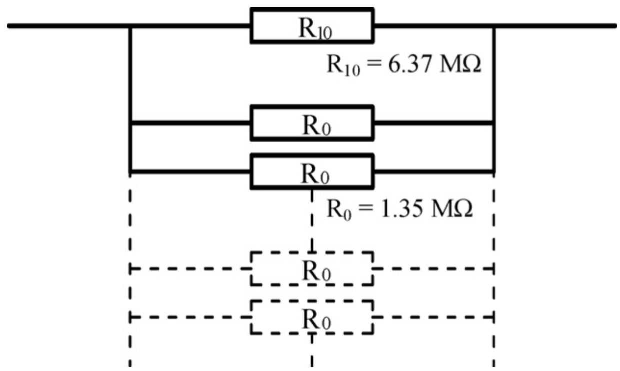

Fig. 5. An equivalent circuit model for the LbL self-assembled SWNT multilayer.

tributes to the conductance of the multilayer. Structurally, the (PDDA/SWNT) bi-layers are parallel to each other. Electrically, they are all connected to the Au electrodes and play similar roles during the carrier transmitting. Compared with SWNTs, the conductivity of PDDA is much lower. SWNT is a highly conductive material with an intrinsic mobility exceeding 100,000 $cm^2/(V\ s)$. On the other hand, PDDA, as the intermediate electrostatic glue, has a high dielectric constant of 30–120 [14]. Therefore, the PDDA layers can be considered as the insulating layers between the SWNT conductive layers. As a result, the SWNT layers can be modeled as a set of resistors in parallel, as shown in Fig. 5. The first 10 SWNT layers are to accumulate SWNTs and provide a conductive channel for the charge carriers. It can be modeled as a "base" resistor with resistance $R_{10} = 6.37\ M\Omega$. The subsequent (PDDA/SWNT) bi-layers can be modeled as "layer" resistors with resistance $R_0 = 1.35\ M\Omega$. The resistance of the SWNT thin-film resistor with n SWNT layers can be calculated as: $R_n = (R_0R_{10})/[R_0 + (n - 10)R_{10}]$. The curve in Fig. 4b represents the theoretical fit from the circuit model. It should be pointed out that the model is built based on empirical observations. Even though the model represents the structural and electrical properties of the multilayer resistors, the data are collected from this particular experiment and the values are only accurate for this type of device. For example, we noticed that the assembly of SWNTs on silicon and flexible substrates can be different. The resulting SWNT films may have different uniformity across the surfaces of the substrates. In general, the SWNT films on silicon substrates have better uniformity. As a result, the film on silicon may need fewer layers to accumulate sufficient SWNTs and provide a channel for charge carriers. In addition, we neglected the interconnection between SWNTs from different layers. This simplifies the model but may not be accurate for certain film configurations. To gain a more thorough understanding of the multilayer films, more data need to be collected and analyzed.

4. Electromechanical characteristics

The effects of the mechanical distortions of carbon nanotubes on their electrical properties have been studied recently [15,16]. One theoretical study shows that the bending of the SWNTs increases their electrical resistance [17]. An *in situ* experiment using AFM tips to deflect individual SWNTs demonstrates that the conductance of the manipulated SWNT can be reduced by two orders of magnitude [18]. Furthermore, a recent electromechanical study shows that the torsional strain on SWNTs can increase the resistance of some tubes but decrease the resistance of others [19]. These theoretical and experimental research efforts provide evidences of individual SWNTs under mechanical distortion. However, it remains uncertain how SWNT composites behave electrically under mechanical deformation. Because of this gap in the research, the electromechanical properties of the LbL self-assembled SWNT thin films are investigated using flexible substrates in this paper. In comparison to silicon substrates, the properties of electrical devices fabricated on flexible polymer substrates are typically less stable and less constant. The resistance of different resistors with the same number of SWNT layers can vary by a large amount. However, the inherent advantage of high flexibility makes the polymer substrates suitable candidates for the electromechanical bending experiments.

The thin-film resistors used in the bending experiments were prepared with the same method described above. They have the same schematic structure as the resistor shown in Fig. 1. The width w is kept as 1 mm and the length l is elongated to 2.8 cm. The measurement system setup is shown in Fig. 6a. One end of the device is fixed on the testing stage. The other end can be moved horizontally toward the fixed end and glued on the testing stage using a double-sided tape at desired locations. During the measurements, the flexible substrate is only allowed to bend upward. The highest point, in the middle of the resistor, is measured and recorded as height, h (in cm). Two testing probes of the HP 4156A are connected to the electrodes and detect the current going through the SWNT resistor. Two resistors with 14 and 16 SWNT layers were characterized; and the

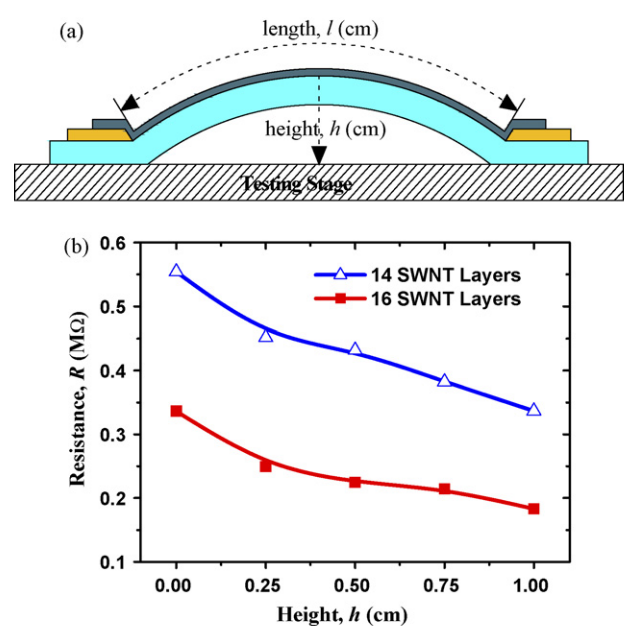

Fig. 6. (a) Electromechanical measurement system setup for the SWNT thin-film resistor on a flexible substrate and (b) resistance vs. mechanical deformation of the SWNT thin films.

resulting height–resistance data are plotted in Fig. 6b. The initial resistances of the flat $(SWNT)_{14}$ and $(SWNT)_{16}$ thin-film resistors are measured as 0.55 and 0.34 MΩ, respectively. For both devices, the resistance decreases with an increased bending height. At the location where $h = 1$ cm, the resistance is measured as 0.34 MΩ for the $(SWNT)_{14}$ resistor and 0.18 MΩ for the $(SWNT)_{16}$ resistor. Here the resistor gain can be defined as $G_n = \Delta R_n/R_n$. Therefore, G_{14} and G_{16} can be calculated approximately as 38.2% and 47.1%, respectively. They are more than 10 times higher than that of silicon (under realistic stress patterns, for p-type silicon, $G \approx 2.8\%$, and for n-type silicon, $G \approx -4.6\%$) [20].

Experimental and theoretical studies from the previous reports revealed that the bending of individual SWNTs decrease its electrical conductance [17,18]. Here, the bulk SWNT composite in these experiments showed an opposite tendency. This can be explained by the nature of the LbL self-assembly and the electromechanical characteristics of the individual SWNTs. One of the main advantages of the LbL self-assembly is that the final structure is close to the thermodynamic equilibrium [21]. The system's thermodynamic minima results in stable and robust structures. Self-assembled materials tend to pack closely to each other and the previous layer. Therefore, the SWNTs bend to follow the topography of the substrate due to their extremely high aspect ratios.

From the SEM inspection, the SWNTs grown by LbL self-assembly are randomly distributed on the surface and overlap each other. Based on the direction of the charge carrier transmission, the SWNTs can be projected into two directions: x-direction which is parallel to it and y-direction which is perpendicular to it. The axial deformation in x-direction has a higher influence on the resistance of the device. Two simplified structural models can be built to represent the SWNT overlapping another SWNT (Model-1) or following a surface with a hole (Model-2), as shown in Fig. 7. The radial deformation of the SWNTs caused by the overlapping is neglected in this model [22].

The SWNTs have high local deformation angles θ_1 and θ_2. When the substrate bends upward at an angle φ, the deformed part of the SWNT remains the same while other parts follow the topography of the bended profile. The SWNTs tend to maximize their adhesion energy and keep the maximum contact area with the substrate [17]. For the Model-1 (Fig. 7b), the local deformation angle decreases to approximately $\theta_1' = \theta_1 - \varphi$. The resistance of the SWNT decreases due to the angle change [18]. For the Model-2 (Fig. 7d), the local deformation angle is approximately $\theta_2' = \theta_2 + \varphi$. The resistance of the SWNT increases due to the angle change. These two effects counteract each other to some extent. The overall resistance is affected by several factors including the magnitude of the angles θ_1, θ_2 and φ; but it mainly depends on which model is the dominant one for most devices. For a perfectly smooth surface with only one SWNT layer, the SWNTs follow the flat surface and bend upward when crossing over another SWNT. Almost all of the axial deformation cases belong to the Model-1, and the Model-2 can be neglected since there is no channel or hole on the surface. For a very rough surface, the possibilities of a SWNT crossing over another SWNT

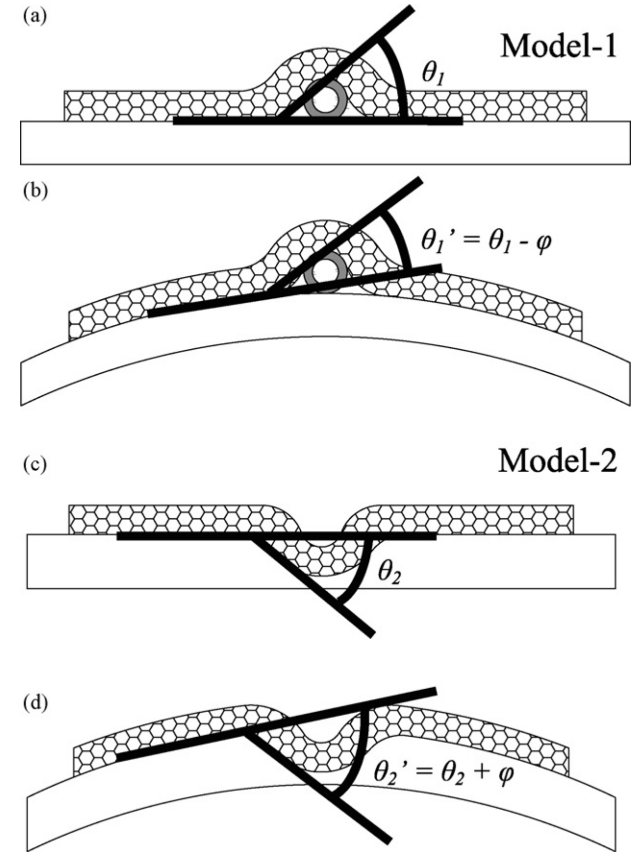

Fig. 7. Schematic models for axial deformation of SWNTs on different topographies.

and falling in a hole are the same. Therefore, these two models are of the same importance. In reality, the LbL self-assembly process provides a relatively smooth surface by using PDDA as the intermediate "annealing" polyelectrolyte [23]. It is unlikely that there are a large number of pits and holes on the surface of the assembled multilayer. Moreover, even though the SWNTs tend to follow the topography of the substrate, fully stretched SWNTs can bridge over small pits and holes without apparent flexure. This reduces the effects of the Model-2. Therefore, the deformed SWNTs represented by the Model-1 have higher effects on the final electrical resistance of the device. In contrast to the electromechanical characteristics of the individual SWNTs, the resistance of the LbL self-assembled SWNT thin-film resistor is decreased when the substrate is bent. However, the underlying principles governing the two phenomena are the same.

It should be pointed out that both models are simplified and can only be used for conceptual demonstration. The models are based on an assumption that the axial deformation of SWNTs is the primary cause for the resistance change. In reality, however, there are many more possibilities. For example, the SWNTs are randomly assembled on the substrate, there is not alignment observed. When bending the flexible substrate, torsional deformation may occur in a number of SWNTs. This may induce resistance change for the SWNT film. As reported by Hall et al., under torsional strain, all metallic and half of the semiconducting SWNTs have resistance increase, while the other half of the semiconducting SWNTs have resistance decrease [19]. Even though it is still uncertain how all the SWNTs perform as a whole in the thin film, we suspect that the two effects counteract each other in some extents and therefore are not the major causes. Another possible cause comes from the nanotube–nanotube interconnection. The bending of the substrate may deteriorate the electrical connection between the SWNTs. In layer-by-layer self-assembled films, however, the SWNTs are always reinforced by two adjacent PDDA layers. The PDDA molecules help the SWNTs to stay in their positions even under substrate bending. Therefore, the nanotube–nanotube interconnection is not considered as the primary cause and it is neglected in the models. To obtain a better understanding of the electromechanical properties of the SWNT thin films, a number of factors such as the axial/radial deformation of the SWNTs, the torsional distortion of the SWNTs, the magnitude of the bending angles, the roughness of the surface, and the nanotube–nanotube interconnection need to be taken into consideration. The simplified models can explain our preliminary experiment results. However, they are not sufficient to explain or predict the value of the resistance shift. In addition to the experimental approach, detailed models consist of all important factors need to be carefully constructed to provide the analytical support.

5. Conclusion

In summary, we have demonstrated the fabrication and characterization of SWNT multilayer thin films on flexible substrates. Measurement of the fabricated resistors shows that the resistance depends highly on the number of SWNT layers. Bending of the substrate can reduce the resistance as much as 47.1%, more than 10 times higher than that of the standard silicon substrates. Based on the unique electromechanical property of the LbL self-assembled SWNT thin films, a number of MEMS/NEMS devices such as pressure sensors, accelerometers, and magnetic sensors can be designed and fabricated.

References

[1] J.W. Judy, Microelectromechanical systems (MEMS): fabrication, design and applications, Smart Mater. Struct. 10 (2001) 1115–1134.

[2] A. Star, J.-C.P. Gabriel, K. Bradley, G. Grüner, Electronic detection of specific protein binding using nanotube FET devices, Nano Lett. 3 (2003) 459–463.

[3] S. Frank, P. Poncharal, Z.L. Wang, W.A. de Heer, Carbon nanotube quantum resistors, Science 280 (1998) 1744–1746.

[4] A. Javey, H. Kim, M. Brink, Q. Wang, A. Ural, J. Guo, P. McIntyre, P. McEuen, M. Lundstrom, H. Dai, High-κ dielectrics for advanced carbon-nanotube transistors and logic gates, Nat. Mater. 1 (2002) 241–246.

[5] T. Dürkop, B.M. Kim, M.S. Fuhrer, Properties and applications of high-mobility semiconducting nanotubes, J. Phys. Condens. Mat. 16 (2005) R553–R580.

[6] E.S. Snow, J.P. Novak, P.M. Campbell, D. Park, Random network of carbon nanotube as an electronic material, Appl. Phys. Lett. 82 (2003) 2145–2147.

[7] J.H. Rouse, P.T. Lillehei, Electrostatic assembly of polymer/single walled carbon nanotube multilayer films, Nano Lett. 3 (2003) 59–62.

[8] A.A. Mamedov, N.A. Kotov, M. Prato, D.M. Guldi, J.P. Wicksted, A. Hirsch, Molecular design of strong single-wall carbon nanotube/polyelectrolyte multilayer composites, Nat. Mater. 1 (2001) 190–194.

[9] E.S. Snow, P.M. Campbell, M.G. Ancona, J.P. Novak, High-mobility carbon-nanotube thin-film transistors on a polymeric substrate, Appl. Phys. Lett. 86 (2005) 033105.

[10] W. Xue, T. Cui, Characterization of layer-by-layer self-assembled carbon nanotube multilayer thin films, Nanotechnology 18 (2007) 145709.

[11] W. Xue, Y. Liu, T. Cui, High-mobility transistors based on nanoassembled carbon nanotube semiconducting layer and SiO_2 nanoparticle dielectric layer, Appl. Phys. Lett. 89 (2006) 163512.

[12] W. Xue, T. Cui, Carbon nanotube micropatterns and cantilever arrays fabricated with layer-by-layer nano self-assembly, Sens. Actuators A 136 (2007) 510–517.

[13] S.M. Sze, VLSI Technology, second edition, McGraw-Hill, Murray Hill, NJ, 1988.

[14] C. Tedeschi, H. Möhwald, S. Kirstein, Polarity of layer-by-layer deposited polyelectrolyte film as determined by pyrene fluorescence, J. Am. Chem. Soc. 123 (2001) 954–960.

[15] S. Paulson, M.R. Falvo, N. Snider, A. Helser, T. Hudson, A. Seeger, R.M. Taylor, R. Superfine, S. Washburn, In situ resistance measurements of strained carbon nanotubes, Appl. Phys. Lett. 75 (1999) 2936–2938.

[16] A. Rochefort, D.R. Salahub, Ph. Avouris, The effect of structural distortions on the electronic structure of carbon nanotubes, Chem. Phys. Lett. 297 (1998) 45–50.

[17] A. Rochefort, Ph. Avouris, F. Lesage, D.R. Salahub, Electrical and mechanical properties of distorted carbon nanotubes, Phys. Rev. B 60 (1999) 13824–13830.

[18] T.W. Tombler, C. Zhou, L. Alexseyev, J. Kong, H. Dai, L. Liu, C.S. Jayanthi, M. Tang, S.-Y. Wu, Reversible electromechanical characteristics of carbon nanotubes under local probe manipulation, Nature 405 (2000) 769–772.

[19] A.R. Hall, M.R. Falvo, R. Superfine, S. Washburn, Electromechanical response of single-walled carbon nanotubes to torsional strain in a self-contained device, Nat. Nanotechnol. 2 (2007) 413–416.

[20] M.J. Madou, Fundamentals of Microfabrication, second edition, CRC Press, Boca Raton, FL, 2002.

[21] Y. Xia, G.M. Whitesides, Soft lithography, Annu. Rev. Mater. Sci. 28 (1998) 153–184.

[22] T. Hertel, R.E. Walkup, Ph. Avouris, Deformation of carbon nanotubes by surface van der Waals forces, Phys. Rev. B 58 (1998) 13870–13873.

[23] G. Decher, Fuzzy nanoassemblies: toward layered polymeric multicomposites, Science 277 (1997) 1232–1237.

Biographies

Wei Xue received the BS and the MS degrees in electrical engineering from Shandong University, Jinan, China, in 1997 and 2000, respectively, and the PhD degree in mechanical engineering from the University of Minnesota, Minneapolis, MN, in 2007. He is currently an assistant professor of mechanical engineering at Washington State University, Vancouver. Before he joined WSU, he was a postdoctoral research associate at the Department of Mechanical Engineering, University of Minnesota. His main research interest includes microfabrication techniques, nanotechnology, polymer/silicon microelectromechanical systems (MEMS), micro/nano electronics, chemical and biological sensors, modeling, and system control.

Tianhong Cui received the BS degree from Nanjing University of Aeronautics and Astronautics in 1991, and the PhD degree from the Chinese Academy of Sciences in 1995. He is currently a Nelson associate professor of mechanical engineering at the University of Minnesota. From 1999 to 2003, he was an assistant professor of electrical engineering at Louisiana Technical University. Prior to that, he was a STA fellow at National Laboratory of Metrology, and served as a postdoctoral research associate at the University of Minnesota and Tsinghua University. He received research awards including the Nelson Endowed Chair Professorship from the University of Minnesota, the Research Foundation Award from Louisiana Tech University, the Alexander von Humboldt Award in Germany, and the STA & NEDO fellowships in Japan. He is a senior member of IEEE and a member of ASME. His current research interests include MEMS/NEMS, nanotechnology, and polymer electronics.